

Lowest Singlet and Triplet States of Copper, Silver, and Gold Trihydrides: an *ab Initio* Study

Nikolai B. Balabanov and James E. Boggs*

*Institute for Theoretical Chemistry, Department of Chemistry and Biochemistry,
The University of Texas at Austin, Texas 78712*

Received: October 25, 2000; In Final Form: April 3, 2001

The lowest singlet and triplet electronic states of CuH_3 , AgH_3 , and AuH_3 were studied. The molecular parameters were optimized at the coupled cluster singles doubles level augmented with perturbative correction for connected triple excitation (CCSD(T)). The equilibrium geometric structures of the lowest singlet states are Y-shaped, with very small values for the valence H–M–H angle. The T-shaped and linear conformations are found to be transition structures. The electronic density and vibrational mode analysis indicates that these molecules can be considered as adducts of a H_2 molecule to the corresponding monohydrides. The lowest triplet states lie $\sim 25\,000$ – $29\,000\text{ cm}^{-1}$ above the minimum of the singlet state. The equilibrium geometry structures of the lowest triplet states are pyramidal with small inversion barriers.

Introduction

Copper, silver, and gold trihydrides represent the simplest examples of three-coordinated compounds of these transition metals. Although the fact that these molecules correspond to the minimum on potential surface has been documented in earlier theoretical studies^{1,2} they have not yet been observed experimentally. In their work using Hartree–Fock (HF) and second-order Møller–Plesset perturbation theory of (MP2) calculations, Swedtfeger et al.¹ found a T-shaped equilibrium structure for singlet AuH_3 . They argued this result was due to the first-order Jahn–Teller effect (the same argument was used by Komya et al.³ to explain a T-shaped structure of the $\text{Au}(\text{CH}_3)_3$ system). Dorigo et al.⁴ (MP2 calculations) reported a similar T-shaped structure of CuH_3 to be a transition state: its negative eigenvalue was pointed out to correspond to a channel for formation of H_2 . Most recently, Bayse and Hall² reported that the Y-shaped structure in AgH_3 and AuH_3 has lower energy than that of the T-shaped one. In the latter study, the geometrical structures and vibrational frequencies were found by the HF method, and then the relative energies were recalculated by single point calculations at the MP2, MP3, and CCSD level.

In view of the difficulty in dealing with these species experimentally, we believe that a clear-cut decision concerning their stabilities, geometries, and transition states from computation is needed. In the present work, we examine the following new questions about the structure of CuH_3 , AgH_3 , and AuH_3 : Does singlet CuH_3 have a Y-shaped minimum like AgH_3 and AuH_3 do? How stable are these molecules with respect to dissociation to the corresponding monohydride and hydrogen? What are the equilibrium structures of these molecules in their lowest triplet electronic states?

Computational Details

Almost all of our calculations were performed using a local version of the ACES II program package.⁵ For copper trihydride,

both all electron (AE) and effective core potential (ECP) calculations were carried out; for silver and gold trihydrides, only ECP calculations were performed. The equilibrium structures and harmonic vibrational frequencies were obtained at the coupled cluster singles doubles level augmented by perturbative correction for connected triple excitation (CCSD(T)).^{6,7} In all-electron calculations, the geometry optimization and harmonic frequencies were computed using analytical gradients and second derivatives of the potential surface.⁸ In ECP calculations, equilibrium geometries were obtained in straightforward energy optimization and vibrational frequencies were determined using second-order finite differences of potential surface.⁵ The relative energies of the triplet excited states of the molecules at their trigonal planar conformations were evaluated by the equation-of-motion coupled cluster method in single and double approximation (EOM-CCSD).⁹ The relative energies of the lowest singlet states in MH_3 ($M = \text{Cu}, \text{Ag}, \text{Au}$) at the D_{3h} structure were computed by the CASSCF method using the GAMESS package.¹⁰ Also, we used the GAMESS program to calculate a minimum energy path on the CuH_3 Jahn–Teller surface at the MP2 level and for calculations of total electron densities of the MH_3 molecules at the ROHF level. The MacMolPlot program¹¹ was used for visualization of the results obtained by the GAMESS program.

$\text{Cu}(14s11p6d1f/10s8p3d1f)$ and $\text{H}(6s3p1d/4s2p1d)$ basis sets were used in all-electron calculations. For copper, we used Wachters basis¹² modified as in the GAMESS program¹⁰ and augmented with a set of f-functions.¹³ The hydrogen basis was the TZ2P set as employed in the ACIS II program expanded with diffuse s-function¹⁴ and second polarization d-functions.¹⁵ The original TZ2P set was the (5s/3s) Dunning set¹⁶ augmented with two optimized p-functions in (2,1) contractions of three primitives.¹⁷

In the ECP calculations, we used two types of effective core potentials on the metal atoms:

SBKJ: The averaged relativistic effective core potentials of Stevens et al.¹⁸ The original valence basis sets¹⁸ were augmented with f-functions^{13,19} and the final basis sets on the metals were

* To whom correspondence should be sent. Fax: 512-471-8696.
E-mail: james.boggs@mail.utexas.edu.

TABLE 1: Parameters of the Y-shaped Structures, Harmonic Vibrational Frequencies, ω_i , of MH_3 ($M = Cu, Ag, Au$)

	CuH ₃			AgH ₃	AuH ₃
	AE ^a	SBKJ ^b	stuttgart ^c	stuttgart	stuttgart
$R_1(M-H_{(1)})$, (Å)	1.488	1.452	1.466	1.593	1.545
$R_2(M-H_{(2)})=R_3(M-H_{(3)})$, (Å)	1.645	1.575	1.639	1.925	1.802
$\alpha(H_{(2)}-M-H_{(3)})$, (deg)	27.6	29.2	27.7	23.1	25.6
$\omega_1(A_1)$	1902	2201	1955	1813	2266
$\omega_2(A_1)$	3779	3676	3766	4012	3614
$\omega_3(A_1)$	892	1228	901	612	804
$\omega_4(B_1)$	1308	1449	1350	977	1420
$\omega_5(B_1)$	427	553	475	406	615
$\omega_6(B_2)$	383	824	555	450	656

^a All-electron CCSD(T) calculations with Cu(14s11p6d1f/10s8p3d1f) and H(6s3p1d/4s2p1d) basis sets. ^b CCSD(T) calculations with SBKJ ECP. ^c CCSD(T) calculations with Stuttgart ECP.

TABLE 2: Parameters of Optimal T-shaped Structures of MH_3 ($M = Cu, Ag, Au$) and Their Relative Energy, ΔE , in Regard to the Y-shaped Structures

parameter	CuH ₃	AgH ₃	AuH ₃
	AE	stuttgart	stuttgart
$R_1(M-H_{(1)})$, (Å)	1.384 ^a	1.479	1.473 ^b
$R_2(M-H_{(2)}) = R_3(M-H_{(3)})$, (Å)	1.492 ^a	1.614	1.613 ^b
$\beta(H_{(1)}-M-H_{(2)}) = \beta(H_{(1)}-M-H_{(3)})$, (deg)	80.2	84.0	87.9 ^b
ΔE , (cm ⁻¹) ^c	12 298	15 137 ^d	9663 ^e
$\omega_1(A_1)$, (cm ⁻¹)	2208	2170	2543
$\omega_2(A_1)$, (cm ⁻¹)	1967	1921	2171
$\omega_3(A_1)$, (cm ⁻¹)	682	758	922
$\omega_4(B_1)$, (cm ⁻¹)	1849	1684	1846
$\omega_5(B_1)$, (cm ⁻¹)	795i ^a	534i	382i
$\omega_6(B_2)$, (cm ⁻¹)	790	943	857

^a $R_1(M-H_{(1)}) = 1.438$ Å; $R_2(M-H_{(2)}) = 1.538$ Å; $\omega_5(B_1) = 981$ cm⁻¹ with the MP2 method⁴. ^b $R_1(M-H_{(1)}) = 1.49$ Å; $R_2(M-H_{(2)}) = 1.65$ Å; $\beta(H_{(1)}-M-H_{(2)}) = 87^\circ$ with the HF method¹. ^c 1 cm⁻¹ = 2.85914 × 10⁻³ kcal/mol = 1.19627 × 10⁻² kJ/mol. ^d 56.14 kcal/mol (19635 cm⁻¹) with the CCSD method². ^e 29.02 kcal/mol (10150 cm⁻¹) with the CCSD method².

TABLE 3: Parameters of Linear Structures of MH_3 ($M = Cu, Ag, Au$) and Their Relative Energy, ΔE , in Regard to the Y-shaped Structures

parameter	CuH ₃	AgH ₃	AuH ₃
	AE	stuttgart	stuttgart
$R_1(M-H_{(1)})$, (Å)	1.471	1.596	1.515
$R_2(H_{(2)}-H_{(3)})$, (Å)	0.742	0.744	0.745
$R_3(M-H_{(2)})$, (Å)	1.761	2.011	2.001
ΔE , (cm ⁻¹)	3502	2108	3572
$\omega_1(\Sigma_g^+)$, (cm ⁻¹)	1881	1744	2300
$\omega_2(\Sigma_g^+)$, (cm ⁻¹)	427	361	379
$\omega_3(\Sigma_g^+)$, (cm ⁻¹)	4411	4378	4367
$\omega_4(\Pi)$, (cm ⁻¹)	176	211	294
$\omega_5(\Pi)$, (cm ⁻¹)	610i	574i	559i

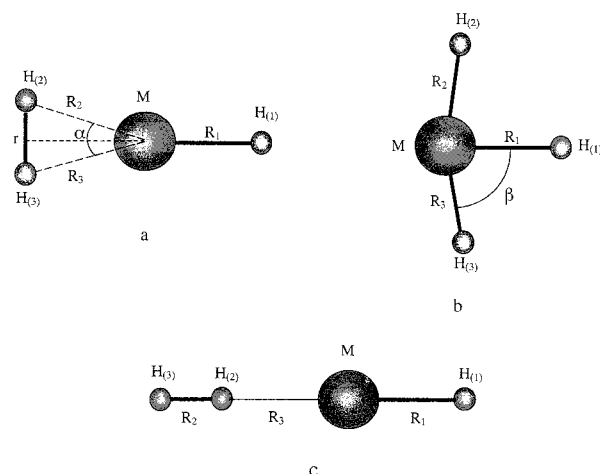
Cu(8s8p6d1f/4s4p3d1f), Ag(7s7p6d2f/4s4p3d2f), and Au(7s7p6d3f/4s4p3d3f).

Stuttgart: The energy-adjusted quasirelativistic pseudopotentials^{20,21} with larger valence basis sets than in SBKJ expanded by polarization f-functions:^{13,19} Cu(8s7p6d1f/6s5p3d1f), Ag(8s7p6d2f/6s5p3d2f) and Au(8s7p6d3f/6s5p3d3f).

In both SBKJ and Stuttgart ECPs the effective core consists of 10 electrons on Cu, 28 electrons on Ag and 60 electrons on Au. The hydrogen basis applied in the ECP calculations was the same as used in all-electron calculations on CuH₃. Spherical d- and f-functions were employed in the CCSD(T) and EOM-CCSD calculations and Cartesian d- and f-functions were applied in the CASSCF and MP2 calculations.

Results and Discussions

Lowest Singlet States. For all molecules, we performed CCSD(T) optimizations of the Y-shaped, T-shaped, and linear H-H-M-H conformations (Figure 1) and characterized them vibrationally. The amplitudes in the CCSD wave functions near

**Figure 1.** Notation of internal coordinates for Y-shaped (a), T-shaped (b), and linear (c) conformations of MH_3 .

the equilibrium structures of the molecules were of small magnitude showing that these molecules can be adequately treated with single reference correlation methods. For example, in the ECP/SBKJ calculations at the equilibrium Y-shaped structures, the maximum T_1 amplitudes of the CCSD wave function were 0.062 in CuH₃, 0.060 in AgH₃, and 0.046 in AuH₃. The maximum T_2 amplitudes were -0.025, -0.041, and -0.034, respectively. The optimal structures are given in Tables 1–3. The Y-shaped structures are “true” minima, whereas linear and T-shaped ones are transition states with one imaginary frequency. The vibrational modes which correspond to their negative eigenvalues are shown in Figure 2(a,b).

The metal–hydrogen distances in MH_3 computed with the SBKJ and Stuttgart effective core potentials differ significantly,

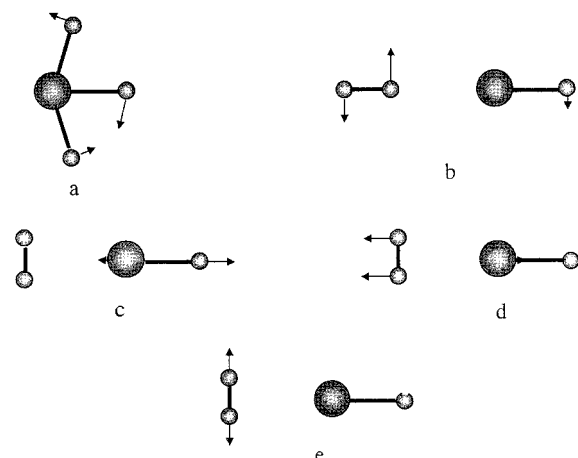


Figure 2. (a) ω_5 (B_1) vibration mode of the T-shaped structure; (b) $\omega_5(\Pi)$ mode of the linear structure; (c), (d), and (e) are $\omega_1(A_1)$, ω_2 (A_1), and $\omega_3(A_1)$ modes of the Y-shaped conformation, respectively.

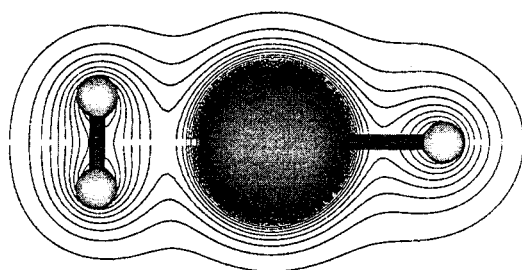


Figure 3. The CuH_3 total electronic density at the ROHF level.

TABLE 4: Parameters of the M–H and H–H Bonds in MH_3 , MH, and H_2

parameter	$\text{H}_2\text{--CuH}$	$\text{H}_2\text{--AgH}$	$\text{H}_2\text{--AuH}$
	AE	stuttgart	stuttgart
$R(\text{M--H})$ in MH_3 , (Å)	1.487	1.593	1.545
$R(\text{M--H})$ in MH, (Å)	1.455 ^a	1.582	1.498
$\omega(\text{M--H})$ in MH_3 , (cm^{-1})	1902 ^b	1813	2070
$\omega(\text{M--H})$ in MH, (cm^{-1})	1906	1763	2357
$R(\text{H--H})$ in MH_3 , (Å)	0.784	0.770	0.800
$R(\text{H--H})$ in MH, (Å)	0.742	0.742	0.742
$\omega(\text{H--H})$ in MH_3 , (cm^{-1})	3779	4012	3614
$\omega(\text{H--H})$ in MH, (cm^{-1})	4410	4410	4410
$R(\text{H}_2\text{--MH})$, (Å)	1.598	1.887	1.757
$\omega(\text{H}_2\text{--MH})$, (Å)	892	612	804
D_e , (cm^{-1})	5280	3158	4478

^a 1.466 Å with MRDCI method,²⁴ 1.457 Å with CASCF + PT2+RC,²⁵ 1.463 Å from experiment.²⁷ ^b 1952 cm^{-1} with MRDCI method,²⁴ 1936.1 cm^{-1} with CASCF + PT2+RC,²⁵ 1940.7 cm^{-1} from experiment.²⁶

by up to 0.06 Å. However, for CuH_3 , the parameters found with the Stuttgart ECP are reasonably close to those obtained in all-electron calculations, which were surely more reliable in this case where relativistic effect are expected to be small. We might therefore assume that the ECP/Stuttgart values of M–H distances for AgH_3 and AuH_3 are also more reliable and only these are given in Tables. As a rule, our calculated structural and energetic parameters are in good agreement with parameters found in previous theoretical studies;^{1,2,4} the relatively large differences of our M–H distances of the T-shaped structure in CuH_3 from those obtained in ref 4 are mostly due to our larger basis sets.

At the MP2/SBKJ level, we calculated the minimum energy path on the hypersurface of the CuH_3 molecule starting from the T-shaped structure and following the imaginary vibrational

TABLE 5: M–H Distances, Valence Angles, Dipole Moments, and Inversion Barriers (h) of MH_3 ($\text{M} = \text{Cu}, \text{Ag}, \text{Au}$) in Their Lowest Triplet State 3A_2

MH_3	$R_e(\text{M--H})$, (Å)	$\alpha(\text{H--M--H})$, deg	$\gamma-90$, deg ^a	μ_z , D	h , cm^{-1}	method
CuH_3	1.511	113.4	15.1	1.208	411	AE
AgH_3	1.642	113.0	15.6	1.025	251	Stuttgart
AuH_3	1.606	117.0	10.0	0.416	103	Stuttgart

^a γ is angle between M–H bond and C_3 symmetry axes in pyramidal structure.

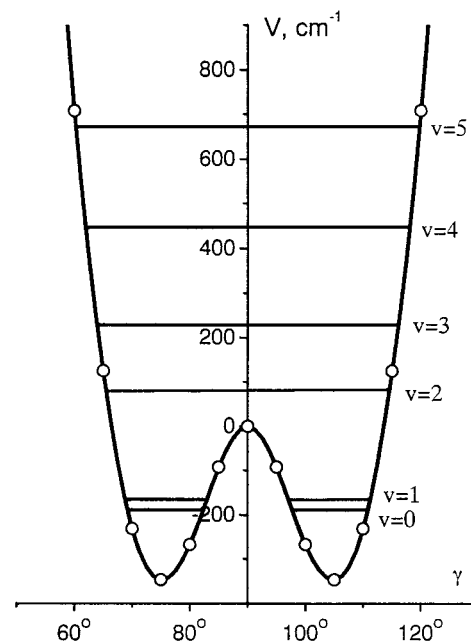


Figure 4. Inversion potential and corresponding vibrational levels of CuH_3 in the lowest triplet electronic states (CCSD(T)/SBKJ level).

mode in the two opposite directions until we reached two equivalent Y-shaped minima. Overall, the potential surfaces of each MH_3 molecule ($\text{M} = \text{Cu}, \text{Ag}, \text{Au}$) have three deep Y-shaped minima separated by three equivalent barriers, which correspond to the T-shaped structures. As described in previous work,^{3,1} such a shape of the potentials surfaces is due to Jahn–Teller distortion^{22,23} of the trigonal planar (D_{3h}) structures of the molecules, which have the degenerate lowest singlet (e'')⁴ (a_1')²(e')²,¹ E' electronic states. The linear H–H–M–H transition structures represent, seemingly, the barriers of the rotation of the H_2 group in the plane of the MH_3 molecules.

The character of the total electron densities of the Y-shaped MH_3 ($\text{M} = \text{Cu}, \text{Ag}, \text{Au}$) molecules indicates that these molecules can reasonably be considered as adducts of H_2 to the corresponding monohydrides. The total electron density of CuH_3 calculated at the ROHF level is presented in Figure 3 as an example. Analysis of the normal coordinates also shows that the ω_1 mode in MH_3 is nearly pure M–H stretching, the ω_2 mode is the stretching between the H_2 group and the MH, and the ω_3 one is H–H stretching inside the H_2 group (see Figure 2 c,d,e). The ω_2 mode leads to the separation of $\text{H}_2\text{--MH}$ to H_2 and MH. At dissociation, the 1A_1 electronic states of MH_3 ($\text{M} = \text{Cu}, \text{Ag}, \text{Au}$) correlate with the $^1\Sigma_g^+$ state of H_2 and the $^1\Sigma^+$ electronic state of the corresponding MH molecule. In CuH , the $^1\Sigma^+$ electronic state is known to be the ground state.^{24,25} We optimized the internuclear distances in the H_2 and MH molecules at the CCSD(T) level and calculated the dissociation energies $D_e = E(\text{MH}) + E(\text{H}_2) - E(\text{MH}_3)$. The results are collected in Table 4 along with the structural and vibrational

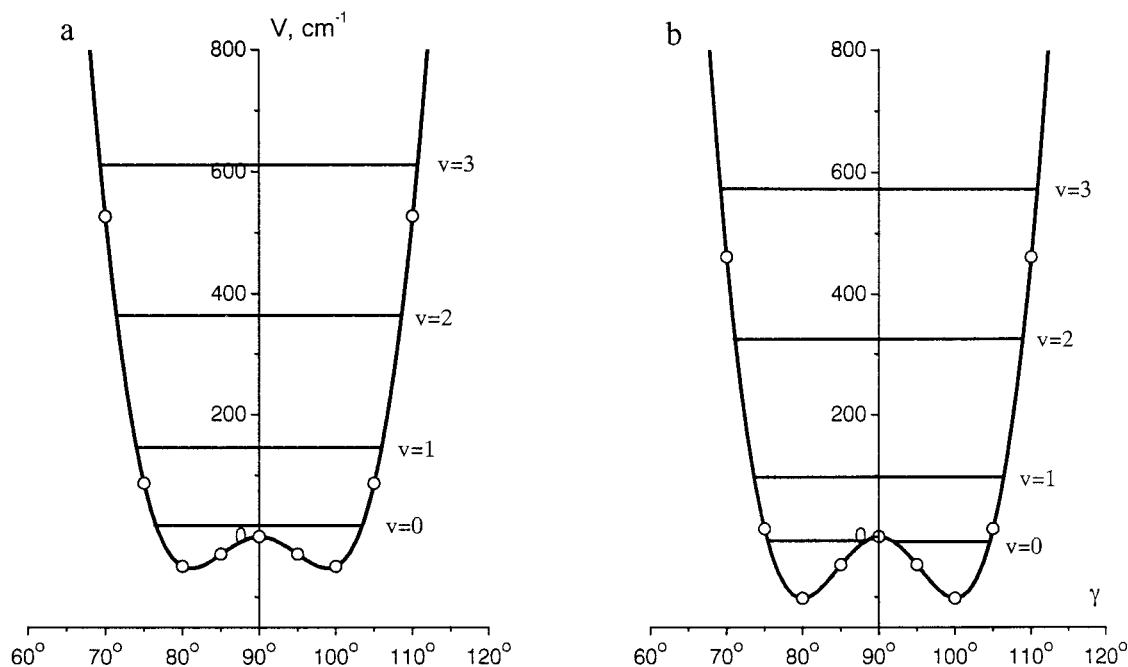


Figure 5. Inversion potentials and corresponding vibrational levels of AuH₃ (a - SBKJ ECP, b - Stuttgart ECP).

TABLE 6: Location of Electronic States in MH₃ (M = Cu, Ag, Au) at Their Trigonal Planar (*D*_{3h}) Conformations

	state	R(M-H), (Å)	ΔE , cm ⁻¹	method
CuH ₃	X ³ A' ₂ , (1e'') ⁴ (3a' ₁) ² (3e') ²	1.515	0	CCSD(T)/AE
	a ¹ E', (1e'') ⁴ (3a' ₁) ² (3e') ²		2742	CASSCF/SBKJ
	A ³ E', (2e'') ³ (3e'') ⁴ (3a' ₁) ² (3e') ³		14 192	EOM-CCSD/AE
	B ³ A'' ₂ , (1e'') ³ (3a' ₁) ² (3e') ³		16 548	EOM-CCSD/AE
AgH ₃	X ³ A' ₂ , (1e'') ⁴ (3a' ₁) ² (3e') ²	1.647	0	CCSD(T)/Stuttgart
	a ¹ E', (1e'') ⁴ (3a' ₁) ² (3e') ²		6193	CASSCF/SBKJ
	A ³ E', (1e'') ⁴ (3a' ₁) ¹ (3e') ³		21 457	EOM-CCSD/Stuttgart
	B ³ A'' ₂ , (1e'') ³ (3a' ₁) ² (3e') ³		33 564	EOM-CCSD/Stuttgart
AuH ₃	X ³ A' ₂ , (1e'') ⁴ (3a' ₁) ² (3e') ²	1.609 ^a	0	CCSD(T)/Stuttgart
	a ¹ E', (1e'') ⁴ (3a' ₁) ² (3e') ²		5418 ^b	CASSCF/SBKJ
	A ³ E', (1e'') ⁴ (3a' ₁) ¹ (3e') ³		26 296	EOM-CCSD/Stuttgart
	B ³ A'' ₂ , (1e'') ³ (3a' ₁) ² (3e') ³		31 042	EOM-CCSD/Stuttgart

^a 1.629 Å with the MP2 method.¹ ^b ~37 kJ/mol (3092 cm⁻¹) with the MP2 method.¹

parameters of MH₃ for comparison. In all our molecules, at least several harmonic vibrational levels that correspond to the ω_2 - (H₂-MH) mode lie below the dissociation level, so the bonding between H₂ and MH (M = Cu, Ag, Au) is quite strong.

For CuH₃, we recalculated the dissociation energy at the all-electron CCSD(T) level with a very large basis set: Cu (21s 15p 10d 6f 4g/8s 7p 5d 3f 2g),²⁷ H (7s 4p 3d 2f/5s 4p 3d 2f).²⁸ The total energies of CuH₃, CuH, and H₂ were calculated at their molecular structures obtained at the CCSD(T) level in the all-electron calculations (Tables 1 and 4). The result was $D_e = 6685$ cm⁻¹ (cf. Table 4). Thus, we can expect that our conclusion about bonding between H₂ and MH would not change significantly with application of a still higher level of theory.

The bonding between H₂ and AgH is the weakest one. The H₂-AgH complex has the smallest dissociation energy and the longest distance between H₂ and MH groups. The addition of H₂ to AgH does not much affect the Ag-H distance. On the other hand, the metal-hydrogen distances in H₂-CuH and H₂-AuH expand by 0.03 and 0.05 Å, respectively. One reason that might be proposed for this effect is the conjecture that the copper and, especially, the gold atom attract more electron charge from molecular hydrogen than silver does and the orbitals in the CuH and AuH molecules, which accept the charge from H₂, have antibonding character. However, the CCSD(T) Mulliken atomic

charges found with different basis sets and ECPs differ significantly and do not support this explanation.

It should be noted that the linear barriers lie below the dissociation limits but the T-shaped barriers are higher than the dissociation energies. Nevertheless, the T-shaped structures are unlikely to be a transition state for the MH₃ → MH + H₂ reaction. The T-shaped conformations do lie on the minimum energy paths which connect two equivalent Y-shaped minima on the hypersurfaces of MH₃ but they do not lie on the shortest minimum energy curve which connects MH₃ with the products H₂ and MH. The reaction MH₃ → MH + H₂ is endothermic but it can go without a barrier.

Lowest Triplet States. At the trigonal planar conformation the lowest electronic state is the triplet (e'')⁴(a'₁)²(e')², ³A'₂. The CCSD(T) energies of the ³A'₂ state relative to the energies of the ¹A₁ singlet states (the Y-shaped structures) are huge: ~27 000 cm⁻¹ in CuH₃, ~29 000 cm⁻¹ in AgH₃ and ~25 000 cm⁻¹ in AuH₃. Calculations of frequencies at the *D*_{3h} conformations show that the planar structures are unstable with respect to out-of-plane deformation. Full optimization leads to the pyramidal equilibrium structures of the molecules; the parameters are given in Table 5. The valence H-M-H angles of the pyramidal structures are close to 120° and the molecules have very small inversion barriers to planarity that decrease the energies of the triplet states only by 100-400 cm⁻¹.

The structures of the triplet states in MH_3 ($M = Cu, Ag, Au$) are similar to the structures of the ground quartet states of MH_3 ($M = Cr, Mo, W$), which were also found to be pyramidal in our previous work.²⁹ The magnitudes of the inversion barriers in the copper family trihydrides are less than those in the chromium group but the trends in the row have the same behavior. The inversion barriers decrease smoothly from CuH_3 to AgH_3 , whereas the valence $H-M-H$ angles decrease from CuH_3 to AgH_3 and increase from AgH_3 to AuH_3 .

The vibrational spectra, which correspond to the inversion $H-M-H$ bending mode were evaluated using the DVR/FBR approach.³⁰ We used the same technique applied to the MH_3 molecules ($M = Cr, Mo, W$),²⁹ with the exception of the calculation of the inversion potentials. The $M-H$ distances change only slightly from the planar to the pyramidal structures of the present series; therefore, we computed the energy of the pyramidal structures with $M-H$ distances fixed to the values of the planar structures. The molecules CuH_3 (Figure 4) and AgH_3 have only two vibrational levels below the inversion barrier. In the AuH_3 molecule, the first level lies near the barrier according to calculations with the Stuttgart ECP and higher than the barrier in calculations with the SBKJ potentials (Figure 5).

The relative energies of the first several excited triplet electronic states were calculated with the EOM-CCSD method using the CCSD wave function of the $^3A'_2$ state as a reference (Table 6). All of them lie quite high relative to the energy of the planar structure of the $^3A'_2$ state. However, the first excited states calculated at their trigonal planar conformations are the singlet $(1e'')^4(3a'_1)^2(3e')^2$, $^1E'$ states, which are Jahn-Teller active. The degenerate $^1E'$ states cannot be treated with single reference methods, therefore their relative energies were evaluated as the difference between the CASSCF energies of the $^1E'$ and $^3A'_2$ states. The CASSCF wave function method consisted of CSFs obtained by distribution of six active electrons on eight active orbitals of $e'', a'_1, e',$ and e' symmetry.

Acknowledgment. This work was supported by a grant from Robert A. Welch Foundation. We are grateful to Prof. John Stanton for the use of his version of ACES II and for helpful discussions.

References and Notes

- Schwerdtfeger, P.; Boyd, P. D. W.; Brienne, S.; Burrell, A. K. *Inorg. Chem.* **1992**, *31*, 3411.
- Bayse, C. A.; Hall, M. B. *J. Am. Chem. Soc.* **1999**, *121*, 1348.
- Komiya, S.; Albright, T. A.; Hoffman, R.; Kochi, J. K. *J. Am. Chem. Soc.* **1976**, *98*, 7255.
- Dorigo, A. E.; Wanner, J.; Schleyer, P. V. *Angew. Chem., Int. Ed. Engl.* **1995**, *34*, 476.
- Stanton, J. F.; Gauss, J.; Watts, J. D.; Lauderdale, W. J.; Bartlett, R. J. *Int. J. Quantum Chem. Symp.* **1992**, *26*, 879.
- Raghavachari, K.; Trucks, G. W.; Pople, J. A.; Head-Gordon, M. *Chem. Phys. Lett.* **1989**, *157*, 479.
- Bartlett, R. J.; Watts, J. D.; Kucharski, S. A.; Noga, J. *Chem. Phys. Lett.* **1990**, *165*, 513.
- Gauss, J.; Stanton, J. F. *Chem. Phys. Lett.* **1997**, *276*, 70.
- Stanton, J. F.; Bartlett, R. J. *J. Chem. Phys.* **1993**, *98*, 7029, and references therein.
- Schmidt, M. W.; Baldrige, K. K.; Boatz, J. A.; Elbert, S. T.; Gordon, M. S.; Jensen, J. H.; Koseki, S.; Matsunaga, N.; Nguyen, K. A.; Su, S. J.; Windus, T. L.; Dupuis, M.; Montgomery, J. A. *J. Comput. Chem.* **1993**, *14*, 1347.
- Bode, B. M.; Gordon, M. S. *J. Mol. Graphics. Mod.* **1999**, *16*, 133.
- Wachtler, A. J. H. *J. Chem. Phys.* **1970**, *52*, 1033.
- Cu f-exponent (3.0) was taken from Baushlicher, C. W.; Roos, B. O. *J. Chem. Phys.* **1989**, *91*, 4785.
- Dunning, T. H.; Hay, P. J. In *Methods of Electronic Structure Theory*; Schaefer H. F., III, Ed.; Plenum press: New York, 1977; Vol. 2. This exponent and some other basis sets and effective core potentials were obtained from the Extensible Computational Chemistry Environment Basis Set Database, Version 1.0, as developed and distributed by the Molecular Science Computing Facility, Environmental and Molecular Sciences Laboratory, which is part of the Pacific Northwest Laboratory, P.O. Box 999, Richland, WA 99352, USA, and funded by the, U.S. Department of Energy. The Pacific Northwest Laboratory is a multi-program laboratory operated by Battelle Memorial Institute for the, U.S. Department of Energy under contract DE-AC06-76RLO 1830. Contact David Feller or Karen Schuchardt for further information.
- Frisch, M. J.; Pople, J. A.; Binkley, J. S. *J. Chem. Phys.* **1984**, *80*, 3265.
- Dunning, T. H. *J. Chem. Phys.* **1971**, *55*, 716.
- Szalay, P. G.; Stanton, J. F.; Bartlett, R. J. *Chem. Phys. Lett.* **1992**, *193*, 573.
- Stevens, W. J.; Krauss, M.; Basch, H.; Jasien, P. G. *Can. J. Chem.* **1992**, *70*, 612.
- Ag f-exponents (2.5 and 0.7) were obtained from Martin, R. J. *J. Chem. Phys.* **1987**, *86*, 5027. Au f-exponents (1.61, 0.68, 0.26) consisted of the three lowest f-exponents from basis listed in Table 3 from work Laerdahl, J. K.; Saue, T.; Faegri, K. Jr. *Theor. Chem. Acc.* **1997**, *97*, 177; truncated to 2 digits after decimal point.
- Dolg, M.; Wedig, U.; Stoll, H.; Preuss, H. *J. Chem. Phys.* **1987**, *86*, 866.
- Andrae, D.; Haussermann, U.; Dolg, M.; Stoll, H.; Preuss, H. *Theor. Chim. Acta* **1990**, *77*, 123.
- Bersuker, I. B.; Polinger, V. Z. *Vibronic Interaction in Molecules and Crystals*; Springer-Verlag: New York, 1989.
- Englman, R. *The Jahn-Teller Effect*; Wiley: New York, 1972.
- Marian, C. M. *J. Chem. Phys.* **1991**, *94*, 5574.
- Pou-Amerigo, R.; Merchan, M.; Nebot-Gil, I.; Malmquist, P. A.; Roos, B. O. *J. Chem. Phys.* **1994**, *101*, 4893.
- Ram, R. S.; Bernath, P. F.; Brault, J. W. *J. Mol. Spectrosc.* **1985**, *113*, 269.
- Pou-Amerigo, R.; Merchan, M.; Nebot-Gil, I.; Widmark, P. O.; Roos, B. O. *Theor. Chim. Acta.* **1995**, *92*, 149.
- Dunning, T. H. *J. Chem. Phys.* **1989**, *90*, 1007.
- Balabanov, N. B.; Boggs, J. E. *J. Phys. Chem. A* **2000**, *104*, 7370.
- Light, J. C.; Hamilton, I. P.; Lill, J. V. *J. Chem. Phys.* **1985**, *82*, 1400.